

Mathematical Proof for the Minimized Stray Fields in Transformers Using Auxiliary Windings Based on State Equations for Evaluation of FEM Results

F. Faghihi and H. Heydari

Abstract: Stray magnetic field is one of the main issues in design of transformers, since it causes non-ideal behavior of transformers. One of the techniques is usually adopted to mitigate the unwanted stray magnetic field is the use of auxiliary windings creating a magnetic field opposite to the incident one giving rise to the reduction of the total magnetic fields. This paper presents a new mathematical proof for optimized parameters such as connection resistance and leakage inductance of the auxiliary windings based on state equations. Some numerical examples for various types of practical transformers are given to demonstrate the validity of the presented mathematical proof and a comparison is made with the results of transformers behavior which is obtained with the help of finite element method. The proposed method is successfully implemented on three different types of transformers: current injection transformer, pulse transformer and superconductor transformers.

Keywords: Characteristics equation, current injection transformer, eigenvalues; finite element method; pulse transformer, superconductor transformer, state equation; stray fields.

1 Introduction

Stray fields provide unsuitable electrical characteristics such as rise time in pulse transformers, AC loss in high temperature superconductive (HTS) transformers, and mechanical force in a 25kA current injection transformer (CIT) [1-5]. According to the influence of stray fields upon these characteristics, so as to achieve better transformer performances a technique adopted to decrease the stray fields, based on the authors' prior arts [4-5]. Two subtractive connected winding can be added to the windings structure of transformers. If these windings are fitted with the same number of turns, the electromotive force generated in the auxiliary windings is due only to the primary and secondary stray field. The current across them produces a magnetic field reducing only the stray fields. As such, considering the effect of the auxiliary windings on the transformer operation, so as to achieve higher performance on the system, different values of auxiliary windings parameters are surveyed.

As a principle object of this paper, a new mathematical proof for the parameters optimization is

presented by obtaining the related dominant poles of the auxiliary windings to be as close to the origin using state equations [7, 8]. Roots of characteristic equation (eigenvalues) for some practical transformers are taken into account for numerical comparisons with finite element method (FEM) results of transformers behavior [9-11].

In the following section, we introduce the differential equations for operating principle of a transformer fitted with two auxiliary windings. In Section 4, new mathematical proof for parameter optimization using state equations is presented. In Section 3, FEM is proposed for results of practical transformers behavior. In section 5, numerical examples are conducted on a real data of three types of transformers and computational comparisons are made with FEM results and recently proposed proof.

2 Preliminary Mathematical Equations for the Physical Concept

In the course of stray field reduction, one solution is to design a new source producing fields opposing the disturbing ones. The new source is designed by two auxiliary windings being wound on the transformer core [6]. In this section, analysis of suggested configuration is presented using theory of electromagnetic coupled circuits.

Iranian Journal of Electrical & Electronic Engineering, 2010.

Paper first received 4 Nov. 2008 and in revised form 12 Jan. 2010.

* The Authors are with the High Voltage and Magnetic Material Research Center, Electrical Engineering Department, Iran University of Science and Technology (IUST), Tehran 1684613114, Iran.

Email: heydari@iust.ac.ir

Consider Fig. 1 as a schematic representation of a mathematical transformer with four windings, where all the windings have positive currents entering their positive terminals, producing magnetic field with the same direction [6, 12].

The instantaneous winding terminal voltages are [6]:

$$v_1 = R_1 i_1 + N_1 \frac{d\phi}{dt} + l_{11} \frac{di_1}{dt} + l_{12} \frac{di_2}{dt} + l_{13} \frac{di_3}{dt} + l_{14} \frac{di_4}{dt} \quad (1)$$

$$v_2 = R_2 i_2 + N_2 \frac{d\phi}{dt} + l_{21} \frac{di_1}{dt} + l_{22} \frac{di_2}{dt} + l_{23} \frac{di_3}{dt} + l_{24} \frac{di_4}{dt} \quad (2)$$

$$v_3 = R_3 i_3 + N_3 \frac{d\phi}{dt} + l_{31} \frac{di_1}{dt} + l_{32} \frac{di_2}{dt} + l_{33} \frac{di_3}{dt} + l_{34} \frac{di_4}{dt} \quad (3)$$

$$v_4 = R_4 i_4 + N_4 \frac{d\phi}{dt} + l_{41} \frac{di_1}{dt} + l_{42} \frac{di_2}{dt} + l_{43} \frac{di_3}{dt} + l_{44} \frac{di_4}{dt} \quad (4)$$

where, N_1, N_2, N_3 and N_4 correspond to the number of winding turns, R_1, R_2, R_3 , and R_4 are the effective resistance of the corresponding windings. l_{jj} and l_{jk} are self-inductance and the mutual inductance coefficients $j, k \in \{1, 2, 3, 4\}$ and ϕ is the resultant field in the core.

According to Eqs. (1)–(4) the instantaneous terminal voltage of each winding is the sum of the winding resistance voltage drop, the induced emf due to the time varying resultant field, and induced electromotive forces associated with the self and mutual stray fields.

Let us consider the transformer supplying power to a load and the auxiliary windings connected as in Fig. 2. In relation to Fig. 1, now $i_2 = -i_o$ where i_o is the load current. The third and fourth windings are connected in subtractive mode. This circuit exemplifies the normal operating condition of the transformer. Considering that, $i_4 = -i_3 = i_{aux}$ in Fig. 2, applying to Eq. (1) through Eq. (4) and taking into consideration that $N_3 = N_4 = N_{aux}$, yields, respectively,

$$v_1 = R_1 i_1 + N_1 \frac{d\phi}{dt} + l_{11} \frac{di_1}{dt} - l_{12} \frac{di_o}{dt} + (l_{14} - l_{13}) \frac{di_{aux}}{dt} \quad (5)$$

$$v_2 = R_2 i_o + N_2 \frac{d\phi}{dt} + l_{21} \frac{di_1}{dt} - l_{22} \frac{di_o}{dt} + (l_{24} - l_{23}) \frac{di_{aux}}{dt} \quad (6)$$

$$v_3 = -R_3 i_{aux} + N_{aux} \frac{d\phi}{dt} + l_{31} \frac{di_1}{dt} - l_{32} \frac{di_o}{dt} + (l_{34} - l_{33}) \frac{di_{aux}}{dt} \quad (7)$$

$$v_4 = R_4 i_{aux} + N_{aux} \frac{d\phi}{dt} + l_{41} \frac{di_1}{dt} - l_{42} \frac{di_o}{dt} + (l_{44} - l_{43}) \frac{di_{aux}}{dt} \quad (8)$$

Given that the third and fourth windings are connected as in Fig. 2, then $v_3 = v_4 - R_a i_a$, which yields:

$$(l_{31} - l_{41}) \frac{di_1}{dt} + (l_{42} - l_{32}) \frac{di_o}{dt} = (R_{aux} - R_a) i_{aux} + l_{aux} \frac{di_{aux}}{dt} - M_{aux} \frac{di_{aux}}{dt} \quad (9)$$

where R_a is the connection resistance and $R_{aux} = R_3 + R_4$ (effective resistance of auxiliary windings), $l_{aux} = l_{33} + l_{44}$ (stray inductance of auxiliary windings) and $M_{aux} = l_{34} + l_{43}$ (mutual inductance of auxiliary windings).

The current passing through the auxiliary windings is governed by Eq. (9). It is interesting to note that i_{aux} is independent of the time derivative of the resultant field, ϕ . As $N_3 = N_4$ then i_{aux} is a consequence of the coupling stray field sharing between N_1 and N_2 stray field encompassing N_3 and N_4 . Moreover, i_{aux} results from the difference between the stray mutual inductance coefficients of N_1 and N_2 with respect to N_3 and N_4 , multiply by the time derivative of the primary and secondary currents. On the other hand, i_{aux} produces a field opposing the primary and secondary stray field.

Referring to Eq. (9), the best way to optimize the operation of the auxiliary windings is to assemble the transformer in such a way that one auxiliary winding is preferentially coupled with the primary and the other is preferentially coupled with the secondary. For example, due to the geometric position of the four windings in the transformer, if we consider that the primary stray field linked preferentially with the third winding and the secondary stray field linked preferentially with the fourth winding, then $l_{31} \square l_{41}$ and $l_{42} \square l_{32}$. These are mathematical analyses which are in quite agreement with the arrangement shown in Fig. 3.

3. Magnetic Field Equations Based on FEM for Practical Results of Transformer Behavior

The practical results are based on the edge element method and mainly magnetic vector potential method. The former method constitutes the theoretical foundation of low frequency electromagnetic field (EMF) element.

The vector potential method is applicable for both 2-D and 3-D EMFs [9, 15-17]. Considering static and dynamic fields and neglecting displacement currents (quasi-stationary limit), the following subset of Maxwell's equations apply [18]:

$$(\nabla \times \{H\} = \{J\}, \nabla \times \{E\} = -\{\frac{\partial B}{\partial t}\}, \nabla \cdot \{B\} = 0.) \quad (10)$$

The basic equation to be solved is in the form of:

$$[\bar{C}] \dot{u} + [K] \{u\} = \{J_i\}. \quad (11)$$

The terms of this equation are defined below; the edge field formulation matrices are obtained from these terms follow with boundary conditions [19, 20].

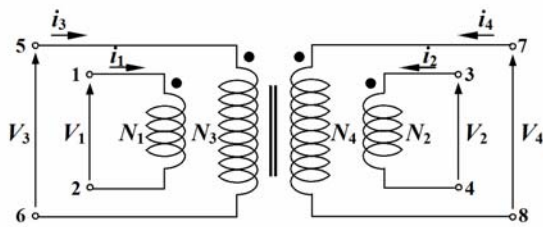


Fig. 1. Schematic representation of the mathematical model of a transformer with four windings

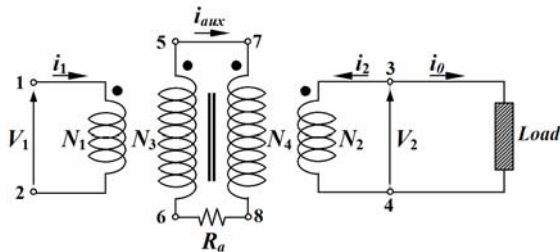


Fig. 2 Schematic representation of the transformer with loaded secondary, N_2 , and the two auxiliary windings connected in subtractive mode, N_3 and N_4

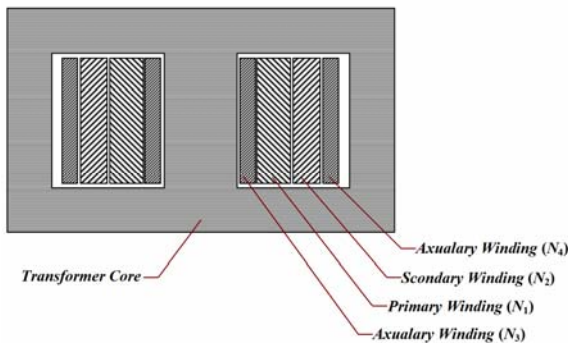


Fig. 3 Simplified layout of new design configuration with the auxiliary windings

4. New Mathematical Proof for Parameter Optimization Using State Equations

With the well known methodology of solving a boundary value problem the determination of the stray magnetic fields in transformers is possible. Taking into account all the Eqs. (5), (6) and (9), the obtained results show the stray fields are reduced. This is achieved by converting the physical model into differential equations in the form of state equations ($\dot{X} = AX + BU, Y = CX$) [13].

Firstly, considering the currents i_1 and i_o are the known values, Eq. (9) can be written in the form of first order linear differential equation:

$$\frac{di_{aux}}{dt} + \frac{R_{aux} - R_a}{L_{aux} - M_{aux}} i_{aux} = f(t) \quad (12)$$

where,

$$f(t) = (l_{31} - l_{41}) \frac{di_1}{dt} + (l_{42} - l_{32}) \frac{di_o}{dt} \quad (13)$$

Homogeneous Response of Eq. (12) is defined as:

$$i_{aux} = k \exp\left[-\frac{R_{aux} - R_a}{L_{aux} - M_{aux}} t\right] \quad (14)$$

where, k is a constant value. The exponential response introduces the time constant criterion in electrical engineering application that illustrates the transient state of system characteristics:

$$\downarrow \tau = \frac{\downarrow (L_{aux} - M_{aux})}{\uparrow (R_{aux} - R_a)} \quad (15)$$

It is well known that by reducing the time constant (τ) faster steady state condition of the system can be achieved. To comply with the above statement, according to Eq. (15) the lowest τ is obtained by the reduction of R_a and L_{aux} . Although the increase of R_{aux} is suitable for better behavior of the system, but the practical consideration such as AC losses makes it unsuitable.

Secondly, roots of characteristic equation of the system are obtained through Laplace transformation using $|sI - A| = 0$ [8]. It is well known that, the rise time analysis of the system depends on the vicinity of negative pole positions to the origin, that is the more vicinity to the origin the faster stability of equation variables (i.e. voltage and current) are achieved [7, 8]. In this case higher reduction of the stray fields in the system occurs. For converting the Eqs. (5) through (8) in the form of the state equation [13, 14], substitution of magnetic field should be done:

$$\varphi = L_{1m} \left[\left(\frac{1}{N_1}\right) i_1 + \left(\frac{N_2}{N_1}\right) i_2 + \left(\frac{N_3}{N_1}\right) i_3 + \left(\frac{N_4}{N_1}\right) i_4 \right] \quad (16)$$

$$L_{1m} = \frac{N_1^2}{\mathfrak{R}_c} \quad (17)$$

where, \mathfrak{R}_c is the reluctance of the magnetic core path and L_{1m} is the magnetizing inductance of the primary winding.

Now, we select the state variables as:

$$\begin{aligned} x_1 &= i_1, \\ x_2 &= i_o, \\ &\bullet \\ x_3 &= x_3, \\ i_{aux} &= x_4, \end{aligned} \quad (18)$$

On the other hand, we have:

$$\begin{bmatrix} \dot{x}_1 \\ \dot{x}_2 \\ \dot{x}_3 \\ \dot{x}_4 \end{bmatrix} = \begin{bmatrix} a_{11} & a_{12} & a_{13} & a_{14} \\ a_{21} & a_{22} & a_{23} & a_{24} \\ a_{31} & a_{32} & a_{33} & a_{34} \\ a_{41} & a_{42} & a_{43} & a_{44} \end{bmatrix} \begin{bmatrix} x_1 \\ x_2 \\ x_3 \\ x_4 \end{bmatrix} + \begin{bmatrix} b_{11} \\ b_{21} \\ b_{31} \\ b_{41} \end{bmatrix} * U \quad (19)$$

$$y = [c_{11} \ c_{12} \ c_{13} \ c_{14}] \begin{bmatrix} x_1 \\ x_2 \\ x_3 \\ x_4 \end{bmatrix} \quad (20)$$

where, U is identity matrix and the coefficients of the A and B matrixes are dependent to the windings characteristics: effective resistance, self and mutual leakage inductance.

$$a_{ij} = f(l_{ij}, R_i, R_a, N_i), \quad i, j \in \{1, 2, 3, 4\} \quad (21)$$

$$b_{ij} = g(l_{ij}, R_i, R_a, N_i), \quad i, j \in \{1, 2, 3, 4\} \quad (22)$$

$$c_{ij} \in \{0, 1\} \quad (23)$$

The above coefficients can be obtained by classical method of the transformer parameter measurements. Each of the coefficients with respect to boundary condition was simply obtained from Eq. (5) through Eq. (8).

The optimum performance of the auxiliary windings adoption in transformers based on the above mentioned criterions for system stability was clarified by solving the state equation corresponding to Eq. (9) for the following cases:

Case 1: for $x_4 = 0$ and $x_4 \neq 0$, the results show that the system is more stable when $x_4 \neq 0$ the roots are nearer to the origin (0,0).

Case 2: the values of $R_a = 0$ and $R_a > 0$ were substituted in a_{ij} and b_{ij} coefficients. The results showed that for $R_a = 0$ the roots are nearer to the origin.

As a consequence, for the investigated method, the auxiliary current i_{aux} must flow through the windings, N_3 and N_4 , with the lowest value R_a in the circuit.

5. Numerical Case studies

For clarity purposes, numerical examples are performed based on the real data obtained from three different types of practical transformers namely: current injection transformer, pulse transformer and superconductor transformers, and are evaluated by computational FEM results.

5.1. Example 1: CIT System

Definition- CIT Systems are within the major group of the standard type test equipments in electrical industry; therefore, their performances are very important. These equipments are able to convert 25A up to 1000A in single-phase or three phases state to high currents (5kA up to 100kA). When designing a high current devices, there are many factors to be considered from which, mechanical forces due to high current passing through secondary winding of the CIT must be ensured. Mechanical forces are highly dependant on the

stray magnetic fields within the windings. The most important parameters of the CIT [3, 9], are shown in Table 1.

FEM results- The proposed method was implemented on a 25 kA-125 kVA single phase CIT. The stray field and mechanical forces in the CIT with and without of the auxiliary windings were simulated using FEM. The results of FEM computations are shown in Tables 2 and 3. These results illustrate that minimum R_a and l_{aux} provide the best operation for the CIT. On the other hand, $R_a = 0 \Omega$, $l_{aux} = 21 \mu H$ are practical optimized parameters in which mechanical force is 691 N. In this condition, peak value of stray flux density is 0.17652T which is the lowest value of stray flux density in this case study.

Table 1 Parameters of the CIT with auxiliary winding

Rating	Capacity Voltage Frequency	125 kVA 400/5 V 50 Hz
Core	Max. Field Density Materials	1.6 T 30 M5
Main Windings	J_c V/T	7.6 A/mm ² 5 V
Auxiliary Winding	J_c No. of Turns	3 A/mm ² 30

Table 2 FEM computation for various values of auxiliary windings resistance (R_a)

Cases	Maximum Stray Flux Density (T)	Mechanical Force (N)
without auxiliary windings	0.20175	1130
with auxiliary windings when $R_a = 0$	0.18225	740
with auxiliary windings when $R_a = 20\Omega$	0.18874	834
with auxiliary windings when $R_a = 50\Omega$	0.19433	976

Table 3 FEM Computation for different stray inductances of auxiliary windings in case of $R_a = 0$

l_{aux} (μH)	Maximum Stray Flux Density (T)	Mechanical Force (N)
37 (conventional design)	0.18225	740
30	0.17954	712
21	0.17652	691

Proposed proof- According to the state Eqs. (18) through (23), calculation of eigenvalues for the CIT system validates the FEM results. The CIT system poles

and the dominant pole for the studied cases are shown in Tables 4 and 5. It is shown in Table 4 the highest rank of the dominant pole belongs to the case with auxiliary windings when $R_a = 0\Omega$ and then for the cases $R_a = 20\Omega$ and $R_a = 50\Omega$, respectively. However, it can be deduced that the short circuited auxiliary windings is the most suitable case for the proposed method. Furthermore, It can be noticed in Table 5 that by reducing the auxiliary windings stray inductances the best condition for CIT operation can be obtained. It can also be seen that, $s_2 = -0.0011 \times 10^4$ (related to $R_a = 0\Omega, l_{aux} = 21\mu H$) is the nearest eigenvalue to the origin compared with the other cases. In this condition the mechanical forces in the FEM results have the lowest values.

Table 4 Computation of system poles for various values of R_a

Cases	System Poles	Dominant Pole
Without auxiliary windings	$s_1 = -1.9313 \times 10^8$ $s_{2,3} = (-0.000029 \pm 0.000861j) \times 10^8$	$s_2 = (-0.000029 - 0.000861j) \times 10^8$
with auxiliary windings when $R_a = 0$	$s_1 = -6.9522 \times 10^4$ $s_2 = -0.0014 \times 10^4$ $s_{3,4} = (-0.1439 \pm 8.9159j) \times 10^4$	$s_2 = -0.0014 \times 10^4$
with auxiliary windings when $R_a = 20\Omega$	$s_1 = -0.0121 \times 10^6$ $s_2 = -6.7036 \times 10^6$ $s_{3,4} = (-0.0018 \pm 0.0437j) \times 10^6$	$s_3 = (-0.0018 - 0.0437j) \times 10^6$
with auxiliary windings when $R_a = 50\Omega$	$s_1 = -0.02765$ $s_2 = -3.2371 \times 10^6$ $s_{3,4} = (-0.0024 \pm 0.0543j) \times 10^6$	$s_3 = (-0.0024 - 0.0543j) \times 10^6$

Table 5 Computation of system dominant poles for different leakage inductances of auxiliary windings in case of $R_a = 0$

l_{aux} [μH]	Dominant pole
37	$s_2 = -0.0014 \times 10^4$
30	$s_2 = -0.0012 \times 10^4$
21	$s_2 = -0.0011 \times 10^4$

5.2. Example 2: Pulse Transformer

Definition- Pulse transformer is a device that is capable of transmitting substantially rectangular voltage pulses, with durations of less than one millisecond.

These devices were developed for applications such as in radar, NLC klystron pulse modulator, driving a microwave amplifier, x-rays for medical and industrial use, gas lasers for plasma technology and plasma immersion ion implantation [1, 2, and 12]. Although several their applications need medium or high voltage pulses (1 up to 700 kV) that medium or high voltage pulse transformer increases the output pulse voltage to the value required for the load. The usually large number of turns in the secondary winding (the transformer ratio is frequently 1:10), together with the insulation gap between windings and within the winding layers give rise to increasing the values of the equivalent parasitic elements (leakage inductance and inter-winding capacitance). These elements speed up the pulse rise time causing overshoot and oscillations [1]. In this case study, the inter-relationship between the pulse rise time and the stray fields are considered by introduction of auxiliary windings in a pulse transformer. Table 6 shows the parameters of the pulse transformer.

Table 6 Parameters of the pulse transformer with auxiliary winding

Rating	Capacity Voltage Frequency	5 kVA 500/5000 V 10 kHz
Core	Max. Field Density Materials	1.5 T 3C85
Main Windings	J_c V/T Inter Winding Capacitance	3 A/mm ² 10 70 pF
auxiliary Winding	J_c No. of Turns	3 A/mm ² 25

FEM results- The proposed method was implemented on a 5 kV-5 kVA single phase pulse transformer. Tables 7 and 8 show the results of the stray field and rise time of the pulse transformer being extracted from FEM calculations for both cases: with and without the auxiliary windings. It is shown in the tables that the best performance of the pulse transformer is obtained when the lowest connection resistance (R_a) and auxiliary windings leakage inductances (l_{aux}) occur. However, from practical point of view $R_a = 0\Omega$ and $l_{aux} = 12\mu H$ are optimized parameters in which the rise time is $7\mu S$ and the peak value of stray flux density is 0.217914 T which is the lowest value in this case study.

Proposed proof- The computations of the eigenvalues for the pulse transformer system validates the FEM results. The poles and the dominant pole for the several values of R_a and l_{aux} are shown in Tables 9 and 10. In this case study, it is shown in Table 9 that the highest rank of the dominant pole ($s_2 = -0.0304 \times 10^4$)

belongs to the case with auxiliary windings when $R_a = 0$ and then for the cases $R_a = 20\Omega$ and $R_a = 50\Omega$, respectively. Furthermore, as it can be seen in Table 10 the reduction of l_{aux} gives the best waveform for the pulse transformer due to the most vicinity of $s_2 = -0.0275 \times 10^4$ (related to $R_a = 0\Omega$ and $l_{aux} = 12\mu H$) to the origin compared to the other cases. As the consequence, the FEM calculated rise time has found to be in its lowest value.

5.3. Example 3: High Temperature Superconductor Transformers

Definition- High temperature superconductor (HTS) transformers promise a variety of benefits, including improving overall power system performance. The specific HTS transformer related benefits include: the ability to overload without loss of insulation life, reduced size and weight, improved efficiency, decreased environmental impact, and ease of siting [11]. Resistive losses in the windings constitute a significant proportion of losses at full load and the desire to further economically reduce these losses using superconducting windings has been an elusive goal for greater than a quarter century [5]. In this case study, the AC losses which highly depend on the stray magnetic flux are considered. The parameters of the studied HTS transformer are shown in Table 11.

Table 7 FEM computation for various values of R_a

Cases	Maximum Stray Flux Density (T)	Rise Time (μ S)
without auxiliary windings	0.43573	36
with auxiliary windings when $R_a = 0$	0.24717	10
with auxiliary windings when $R_a = 20\Omega$	0.26901	14
with auxiliary windings when $R_a = 50\Omega$	0.29728	17

Table 8 FEM Computation for different leakage inductances of auxiliary windings in case of $R_a = 0$

l_{aux} (μ H)	Maximum Stray Flux Density (T)	Rise time (μ S)
19 (conventional design)	0.24717	10
15	0.22763	8
12	0.217914	7

Table 9 Computation of system poles for various values of R_a

Cases	System poles	Dominant pole
without auxiliary windings	$s_1 = -2.3371 \times 10^8$ $s_{2,3} = (-0.000441 \pm 0.000096j) \times 10^8$	$s_2 = (-0.000441 - 0.000096j) \times 10^8$
with auxiliary windings when $R_a = 0$	$s_1 = -2.5925 \times 10^4$ $s_2 = -0.0304 \times 10^4$ $s_{3,4} = (-0.3572 \pm 2.1631j) \times 10^4$	$s_2 = -0.0304 \times 10^4$
with auxiliary windings when $R_a = 20\Omega$	$s_1 = -3.878 \times 10^6$ $s_2 = -6.4252 \times 10^6$ $s_{3,4} = (-0.0725 \pm 0.2561j) \times 10^6$	$s_3 = (-0.0725 - 0.2561j) \times 10^6$
with auxiliary windings when $R_a = 50\Omega$	$s_1 = -1.0025 \times 10^6$ $s_2 = -3.6821 \times 10^6$ $s_{3,4} = (-0.0992 \pm 0.0882j) \times 10^6$	$s_3 = (-0.0992 - 0.0882j) \times 10^6$

Table 10 Computation of system dominant poles for different leakage inductances of auxiliary windings in case of $R_a = 0$

l_{aux} (μ H)	Dominant pole
19	$s_2 = -0.0304 \times 10^4$
15	$s_2 = -0.0289 \times 10^4$
12	$s_2 = -0.0275 \times 10^4$

Table 11 Data of the HTS transformer with auxiliary winding

Rating	Capacity Voltage Frequency	20 kVA 400/220 V 50 Hz
Core	Max. Field Density Materials	1.6 T 30M5
Main Windings	Material J_c V/T	BSCCO tape 18 A/mm ² 4.5 V
auxiliary Winding	Material J_c No. of Turns	BSCCO tape 18 A/mm ² 35

FEM results- The auxiliary winding technique was also performed for a 220 V-20 kVA single phase HTS transformer. The stray flux density and AC losses of the HTS transformer for both cases: with and without the auxiliary windings, were calculated by FEM. The results of FEM computations are shown in Tables 12 and 13. These results show that the AC losses are in its lowest value (due to the lowest stray field) are achieved

when the auxiliary windings parameters are the lowest. It can be concluded that, the best case is when $R_a = 0\Omega$ and $l_{aux} = 6\mu H$ from which AC loss is 3.19 W.

Table 12 FEM computation for various values of R_a

Cases	Maximum Stray Flux (T)	AC Loss (W)
without auxiliary windings	0.03782	4.75
with auxiliary windings when $R_a = 0$	0.03459	3.54
with auxiliary windings when $R_a = 10\Omega$	0.03586	3.87
with auxiliary windings when $R_a = 20\Omega$	0.03643	4.14

Table 13 FEM Computation for different stray inductances of auxiliary windings in case of $R_a = 0$

l_{aux} (μH)	Maximum Stray Flux Density (T)	AC Loss (W)
12	0.03459	3.54
8	0.03395	3.32
6	0.03243	3.19

Table 14 Computation of system poles for various states of R_a

Cases	System poles	Dominant pole
without auxiliary windings	$s_1 = -1.3451 \times 10^8$ $s_{2,3} = (-0.000061 \pm 0.000652j) \times 10^8$	$s_2 = (-0.000061 - 0.000652j) \times 10^8$
with auxiliary windings when $R_a = 0$	$s_1 = -6.6801 \times 10^4$ $s_2 = -0.0552 \times 10^4$ $s_{3,4} = (-0.5674 \pm 5.1431j) \times 10^4$	$s_2 = -0.0552 \times 10^4$
with auxiliary windings when $R_a = 10\Omega$	$s_1 = -4.5671 \times 10^6$ $s_2 = -6.0037 \times 10^6$ $s_{3,4} = (-0.0627 \pm 0.0313j) \times 10^6$	$s_3 = (-0.0627 - 0.0313j) \times 10^6$
with auxiliary windings when $R_a = 20\Omega$	$s_1 = -4.2541 \times 10^6$ $s_2 = -2.4319 \times 10^6$ $s_{3,4} = (-0.0825 \pm 0.0782j) \times 10^6$	$s_3 = (-0.0825 - 0.0782j) \times 10^6$

Table 15 Computation of system dominant poles for different leakage inductances of auxiliary windings in case of $R_a = 0$

l_{aux} (μH)	Dominant pole
12	$s_2 = -0.0552 \times 10^4$
8	$s_2 = -0.0462 \times 10^4$
6	$s_2 = -0.0417 \times 10^4$

Proposed proof- Calculation of eigenvalues for the HTS transformer validates the FEM results. The poles and the dominant pole for the above mentioned cases are shown in Tables 14 and 15. According to Table 14, the highest rank of the dominant pole belongs to the case with auxiliary windings when $R_a = 0$ and then for the cases $R_a = 10\Omega$ and $R_a = 20\Omega$, respectively. Moreover, FEM calculation shows that minimized AC loss is related to the conditions in which $R_a = 0\Omega$ and $l_{aux} = 6\mu H$ that is in good agreement with the results shown in Table 15.

6. Conclusion

In this paper the dominant effects of the stray fields influencing mechanical forces in CIT, pulse rise time in pulse transformers and AC losses in HTS transformers, have been thoroughly investigated. In each case study, the stray fields were calculated in the presence and absence of auxiliary windings by FEM analysis and the corresponding results were validated with the proposed mathematical proofs of the concept. The mathematical proofs were based on related dominant poles of the auxiliary windings to be as close to the origin as possible using state equations.

The present approach has been described with reference to exemplary embodiments. However, it will be readily apparent to those skilled in the art that it is possible to embody the phenomena in the other electromagnetic systems other than those three case studies described above without departing from the spirit of the concept.

Acknowledgments

The financial support of the Tehran Regional Electric Company; Energy Ministry of Iran is gratefully acknowledged.

References

- [1] Gollor M. and Schaper W., "Design of a 130 kV Pulsed Power Supply for a Space Based CO₂ Laser", *IEEE Pulsed Power Conference*, Vol. 2, pp. 934-939, 1995.
- [2] Koontz R., Akemoto M., Gold S., Kransnykh A. and Wilson Z., "NLC Klystron Pulse Modulator R&D AT SLAC", *Proceedings IEEE Conference on Magnetics*, pp. 1319-1321, 1998.
- [3] Heydari H. and Pedramrazi S. M., "Impact of Mechanical Forces in a 25 kA Current Injection

- Transformer”, *Iranian Journal of Engineering Sciences (IJES)*, Vol. 1, No. 1, December 2007.
- [4] Heydari H. and Faghihi F., “Hybrid Winding Configuration in High Current Injection Transformers Based on EMC Issues”, *IET Electr. Power Appl.*, Vol. 3, No. 3, pp. 187–196., 2009.
- [5] Heydari H., Faghihi F. and Aligholizadeh R., “A New Approach for AC loss Reduction in HTS Transformer Using Auxiliary Windings: Case Study 25 kA HTS Current Injection Transformer”, *Supercond. Sci. Technol.*, 21, pp. 1-6, 2008.
- [6] Lipschutz S. and Lipson M., *Linear Algebra*, Schaum’s outlines, third edition, 2000.
- [7] Chen B. M., Lin Z. and Shamash Y., *Linear System Theory*, Birkhauser, 2004.
- [8] Heydari H., Ariannejad M. and Faghihi F., “Simulation and Analysis of 25 kA Current Injection Transformer (CIT) with Finite Element Method”, *IEEE Conference MELECON*, pp. 909-915, 2004.
- [9] Sadedin D. R., “Geometry of a Pulse Transformer for Electromagnetic Launching”, *IEEE Transactions on Magnetics*, Vol. MAG-20, No. 2, pp. 381-384, 1984.
- [10] Funaki K, et al., “Preliminary Tests of a 500 kVA-Class Oxide Superconducting Transformer cooled by Subcooled Nitrogen”, *IEEE Trans. Appl. Supercond.*, Vol. 7, pp. 824–827, 1997.
- [11] Redondo L. M., Margato E. and Silva J. F., “Rise Time Reduction in High Voltage Pulse Transformers Using Auxiliary Windings”, *IEEE Transactions on Power Electronics*, Vol. 17, No. 2, pp. 196-206, 2002.
- [12] Qiu Y., Zhang Z. and Lu J., “The Matrix Equations $AX=B$, $XC=D$ with $PX=sXP$ Constraint”, *Applied Mathematics and Computation*, Vol. 189, No. 2, pp. 1428-1434, 2007.
- [13] Zhang Z. Y. and Zhang H. S., “Calculation of Eigenvalue and Eigenvector Derivatives of a Defective Matrix”, *Applied Mathematics and Computation*, Vol. 176, No. 1, pp. 7-26, 2006.
- [14] Sadiku and Matthew, *Numerical Techniques in Electromagnetic*, Second Edition, CRC Press, 2001.
- [15] Bedrosian G., “High-Performance Computing for Finite Element Methods in Low-Frequency Electromagnetics”, *Progress In Electromagnetics Research*, PIER 07, pp. 57-110, 1993.
- [16] Gross P. W. and Kotiuga P. R., “Data Structures for Geometric and Topological Aspects of Finite Element Algorithms”, *Progress In Electromagnetics Research*, PIER 32, pp. 151-169, 2001.
- [17] Li J. S., Yu Z. Y., Xiang X. Q., Ni W. P. and Chang C. L., “Least-Square Finite Element Method for Electromagnetic Fields in 2-D”, *Applied Mathematics and Computation*, Vol. 58, No. 2-3, pp. 143-167, 1993.
- [18] Chang C. L., “Finite Element Method for the Solution of Maxwell’s Equations in Multiple Media”, *Applied Mathematics and Computation*, Vol. 25, No. 2, pp. 89-99, 1988.
- [19] Ma C. and Wang D., “Finite Element Analysis of an A- Φ Method for Time-Dependent Maxwell’s Equations Based on Explicit-Magnetic-Field Scheme”, *Applied Mathematics and Computation*, Vol. 190, No. 2, pp. 1273-1283, 2007.



Faramarz Faghihi obtained the B.Sc. degree in Electrical Engineering from university of Tehran, Iran, in 2000 and then an M.Sc in communication engineering from Imam Hossein University, Tehran, Iran, in 2002. A PhD in Current Injection Transformer Optimization at IUST in July 2008. His research interests are EMC, Transformers and Superconductors.



Hossein Heydari obtained the B.Sc. degree on Electrical Engineering in 1985 and then an M.Sc in Power Electronic at Loughborough University in 1987. A PhD in transformer core losses at University of Wales in 1993. Following graduation, he was employed by IUST as an academic member (Lecturer) of Electrical Power group and he also was appointed as the Director of High Voltage & Magnetic Materials Research Center. His lecture duties are: Electrical Machines, Electrical Measurement and Instrumentations and EMC Applications in Electrical Power Systems. His research interests are in EMC Considerations in Electrical Power Systems, Fault Current Limiters, Superconductors, Electrical Machine Core Losses.